CivilEng

MDPI

Article

Neural Network Prediction and Enhanced Strength Properties of Natural Fibre-Reinforced Quaternary-Blended Composites

Pavithra Chandramouli [1], Mohamed Riyaaz Nayum Akthar [2], Veerappan Sathish Kumar [3,*], Revathy Jayaseelan [2,*] and Gajalakshmi Pandulu [2]

[1] Department of Civil Engineering, Faculty of Engineering and Technology, SRM Institute of Science & Technology, SRM Nagar, Kattankulathur 603203, Tamil Nadu, India; pavithrc@srmist.edu.in
[2] Department of Civil Engineering, B. S. Abdur Rahman Crescent Institute of Science & Technology, Chennai 600048, Tamil Nadu, India; riyaaz97@gmail.com (M.R.N.A.); gajalakshmi@crescent.education (G.P.)
[3] Department of Civil Engineering, National Institute of Technology Puducherry, Karaikal 609609, Puducherry, India
* Correspondence: vsk.civil@nitpy.ac.in (V.S.K.); revathyj@crescent.education (R.J.)

Abstract: This research, with its potential to revolutionise the construction industry, aims to develop quaternary-blended composites (QBC) by replacing 80% of ordinary Portland cement (OPC) with metakaolin, rice husk ash, and wood ash combined with discrete hybrid natural fibres at a volume fraction of 0.5%. This study investigates the mechanical properties, including compressive strength, split tensile strength, and impact strength of the QBC at various curing ages of 7, 28, and 56 days. Scanning electron microscopy (SEM) analysis was performed to assess the microstructural characteristics. This research aimed to formulate a novel quaternary binder that may minimise our reliance on cement. The experimental results indicate that the mix labelled M4L2 exhibited superior compressive and split tensile strength performance, with percentage increases of approximately 51.03% and 29.19%, respectively. Meanwhile, the M5L1 mix demonstrated enhanced impact energy, with a percentage increase of about 36.40% in 56 days. SEM observations revealed that the MC4 mix contained unhydrated portions and larger cracks. In contrast, the presence of fibres in the M4L2 mix contributed to crack resistance, resulting in a denser matrix and improved microstructural properties. This study also employed an artificial neural network (ANN) model to predict the compressive, tensile, and impact strength characteristics of the QBC, with the predictions aligning closely with the experimental results. An investigation was conducted to determine the ideal number of hidden layers and neurons in each layer. The model's effectiveness was evaluated using statistical metrics such as correlation coefficient (R), coefficient of determination (R^2), root mean square error (RMSE), mean absolute error (MEA), and mean absolute percentage error (MAPE). The findings suggest that the developed QBCs can effectively reduce reliance on conventional cement while offering improved mechanical properties suitable for sustainable construction practices.

Keywords: quaternary blends; SCM; fibres; RHA; metakaolin; wood ash; ANN; synergic effect

Citation: Chandramouli, P.; Akthar, M.R.N.; Kumar, V.S.; Jayaseelan, R.; Pandulu, G. Neural Network Prediction and Enhanced Strength Properties of Natural Fibre-Reinforced Quaternary-Blended Composites. *CivilEng* **2024**, *5*, 827–851. https://doi.org/10.3390/civileng5040043

Academic Editors: Ying Huang and Angelo Luongo

Received: 8 August 2024
Revised: 14 September 2024
Accepted: 18 September 2024
Published: 26 September 2024

1. Introduction

In recent years, climate change and resource depletion have drawn more attention. Ordinary Portland cement (OPC) is a key ingredient of the concrete to act as a hydraulic binder. However, it is still extensively utilised, and its production poses severe environmental problems by producing a large quantity of CO_2 in the atmosphere. It has been reported that 1 tonne of cement releases 0.87 tonnes of carbon dioxide [1,2]. Industrial waste must be disposed of safely to protect the environment. Agro-based waste disposal also harms the environment. Over 600 MT of agro-based trash is produced in India [3]. Sustainable concrete materials are a priority in the building industry. By using industrial and agro-based wastes with pozzolanic behaviour, concrete manufacturing could change significantly. The supplementary cementitious materials (SCMs) from industrial wastes such fly ash (FA),

ground granulated blast furnace slag (GGBS), silica fume, metakaolin (MK), and agro-based wastes like rice husk ash (RHA), sugarcane bagasse ash, groundnut shell, coconut shell, and sawdust. SCMs are rich in silica, calcium oxide, and alumina. Pozzolanic substance can replace cement in concrete manufacture. Thus, it lowers carbon footprint and material production costs [4–7]. Studies show that SCMs improve concrete's mechanical and durability properties [8,9]. Several studies found that OPC with industrial and agro-based wastes influenced cement or concrete behaviour. MK greatly enhanced binary blend workability. Binary mixtures in concrete utilise more cement and thus may be expensive [10,11]. FA significantly enhanced slump flow diameter in binary blends, but metakaolin decreased it. FA and MK in ternary mixes reduced setting time [12]. As grinding time increased, RHA particle size decreased. Grinding increases material pozzolanic activity [13]. The combined usage of cement, FA and RHA/bagasse ash reduced the porosity of mortar [14]. Researchers are showing interest in the utilisation of bottom ash in concrete production. The ultra-fine coal bottom ash blended with cement showed an increase in workability and setting time [15]. Ternary blends are more effective than binary blends because they limit corrosion; hence, using additional RHA reduces strength [16]. Self-compacting concrete compositions using ternary blends of oil palm fuel ash, FA, and hybrid-blended aggregates had decreased calcium hydroxide and ettringite formation [17]. The development of quaternary-blended cementitious materials is an innovative step in the construction industry. While binary and ternary blends have been studied extensively, quaternary blends offer a new frontier with the potential for enhanced performance characteristics. For self-compacting concrete (SCC), quaternary blending of cement with mineral admixtures was tested. Binary and ternary blend with cement, slag, and silica fume demonstrated better compressive strength than fly ash-incorporated concrete. Quaternary cement–mineral admixtures reduced SCC sorptivity [18]. Choudhary et al. studied the quaternary influence of marble slurry waste, fly ash, and silica fume [19]. The microstructure analysis showed that the mortar matrix was dense, improved the packing of aggregate, and had fewer voids [20]. The synergy of different SCMs in cementitious materials would enhance the strength properties of concrete [21,22]. From past studies, adding SCMs to concrete reduces the amount of cement needed—but the unreinforced system may fracture at low strain capacity—which greatly improves concrete properties with discrete fibres [23]. The discrete hybrid fibres in concrete showed potential benefits over the mono discrete fibres. From the literature, a variety of hybrid discrete fibres incorporated in concrete enhance the properties of concrete [24–26]. Natural fibre composite (NFC) research and innovation are cheaper and more environmentally friendly than synthetic fibre composites, which supports their use in diverse fields [27]. The combination of fibres with quaternary blends offers a novel approach to addressing the limitations of traditional concrete, such as susceptibility to cracking, limited durability, and a high environmental footprint. The use of fibres improves tensile strength, flexural strength, and impact resistance, which are critical for structural applications. The quaternary blend further enhances these properties by optimising the microstructure and reducing porosity [28]. Soft computing tackles complicated issues cost-effectively. Artificial neural networks (ANNs) mimic human neurons. They have three layers—input, hidden, and output—connected by brain-like neurons. Civil engineers are increasingly using ANNs to address several difficulties [29]. ANNs can understand complicated variables from training data, making them a prominent deep learning application for regression [30]. Researchers use machine learning to manage metadata-rich datasets with various calculations [31]. Several research studies have been investigated for predicting the workability [32], strength properties [33], and durability properties [34] of normal and high-strength concrete [35], binary and ternary blended concrete [36], high-performance concrete [37], fibre reinforced concrete [38], geopolymer concrete [39,40], as well as the load-carrying capacity of structural members [41,42]. ANNs can eliminate the need for extensive experimental work. This approach offers significant advantages in saving time, reducing costs, and minimising labour [43]. In summary, this work contributes to sustainable construction and predictive modelling by targeting environmental issues,

the progress of quaternary-blended composites, and harnessing the capabilities of artificial intelligence [44].

In this study, cementitious materials rich in silica and calcium oxide from agro-industrial wastes were utilised to reduce the amount of OPC needed. RHA, WA, and MK were replaced with OPC to make quaternary-mixed cementitious materials. Fibre-reinforced quaternary-blended composites were developed from these blended cementitious materials with discrete hybrid natural fibres. Furthermore, we analysed RHA, WA, and MK efficiency factors on which Bolomey's equation could calculate compressive strength. This work also creates an ANN model to predict QBC compressive, split tensile, and impact energy.

2. Materials and Methods

2.1. Materials

The materials used in the present work are ordinary Portland cement of 53 grade, confirming IS 12269: 2013 [45]. The physical and chemical properties of OPC, MK, RHA, and WA are presented in Table 1. Figure 1a–d show SEM images of the cement and SCM materials. The SEM image exhibits the irregular shape of the cement particles and coarser particles in metakaolin. A porous surface with an irregular shape is noticed in RHA, whereas a rough and smooth surface with an irregular shape is observed in wood ash. Metakaolin and RHA particles are found to be smaller than cement particles. Locally available river sand of zone II, confirming to IS 383 [46], was used as fine aggregate. The physical properties of fine aggregate were tested as per IS 2386 (Part 3) [47], and the results of specific gravity, fineness modulus, bulk density, water absorption, and moisture content were 2.64, 2.58, 1510 kg/m^3, 0.80%, and 6% respectively.

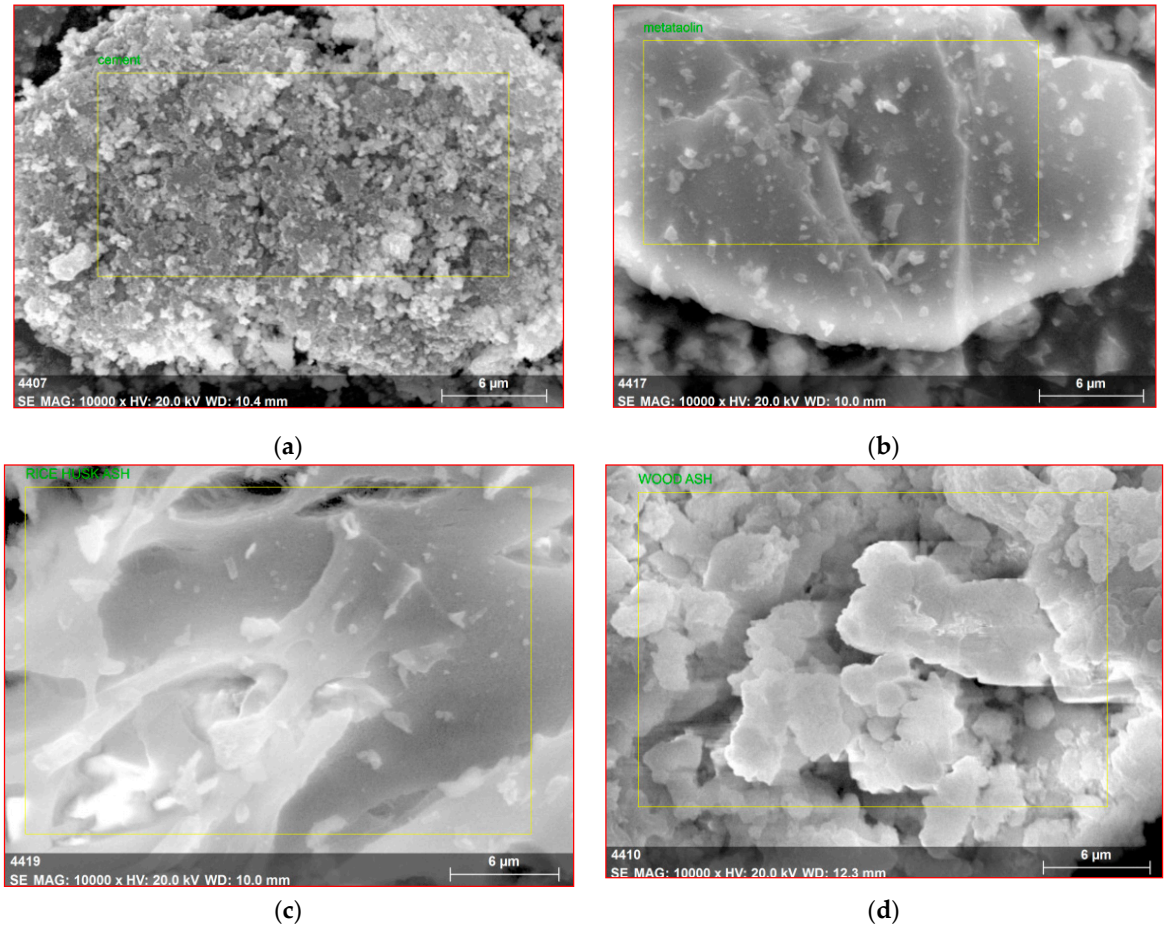

Figure 1. SEM images: (**a**) ordinary Portland cement; (**b**) metakaolin; (**c**) rice husk ash; (**d**) wood ash.

Table 1. Physical and Chemical Composition of OPC, MK, RHA, and WA.

	OPC	MK	RHA	WA
Physical Properties				
Specific gravity	3.14	2.30	2.14	1.71
Specific surface area (cm^2/g)	2285	8735	3750	1203
Mean particle size (μm)	90	2	4	180
Chemical Composition (%)				
SiO_2	20.38	55.25	97.32	9.29
CaO	71.60	0.40	---	58.27
Na_2O	0.18	0.18	0.26	6.96
K_2O	0.09	1.40	--	3.95
Al_2O_3	3.22	44.14	0.20	3.03
FeO	2.88	0.09		7.68
MnO	0.07	0.08	0.01	0.24
MgO	0.98	0.08	0.21	5.03
TiO_2	0.29	---	0.19	0.27
SO_3	0.26	---	---	2.88
P_2O_5	0.05	---	---	0.62
ZnO	---	---	---	---
LoI	2.20	0.25	4.0	20.1

2.2. Processing and Properties of Natural Fibres

The locally available banana and jute fibres were used in this study. The banana and jute fibres were treated using a 5% sodium hydroxide (NaOH) solution for 2 h [48]. The alkaline treatment process of banana and jute fibres is represented in the flow chart, as shown in Figure 2a. The fibres were cut into two different lengths of 10 mm and 20 mm. Figure 2b,c depict processed, cut banana, and jute fibres of various lengths. The salient properties of the fibres are presented in Table 2.

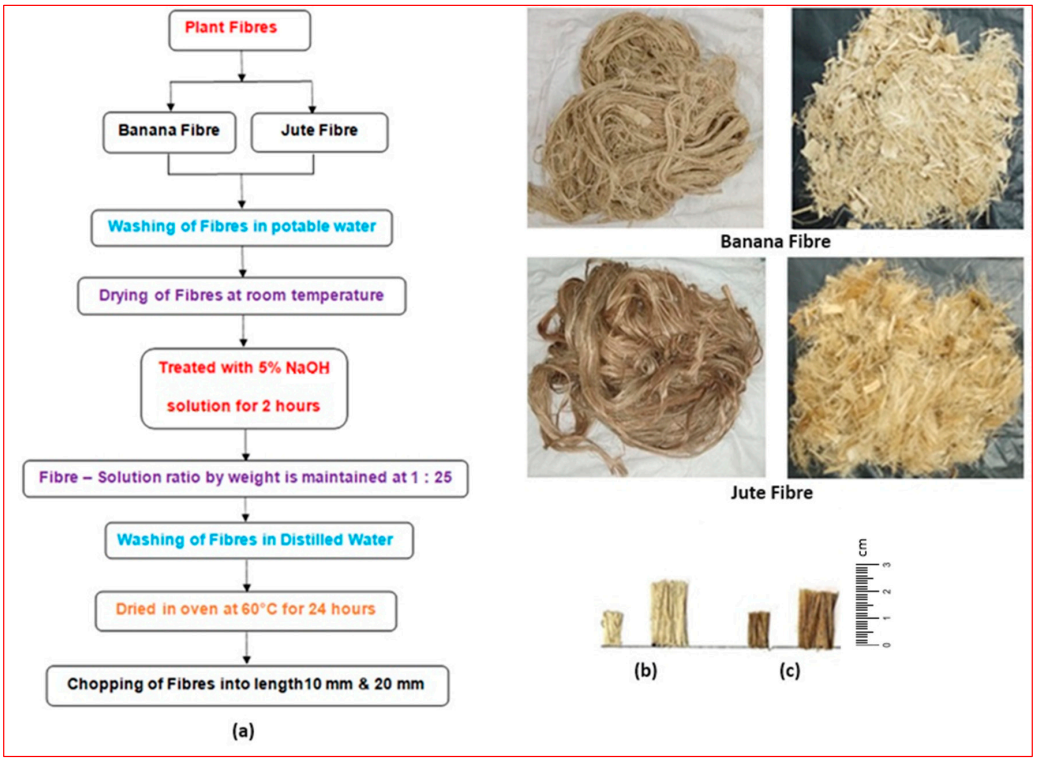

Figure 2. (**a**) Fibre processing procedure; (**b**) processed cut banana fibre; (**c**) processed cut jute fibre.

Table 2. Properties of natural fibres.

Plant Fibre Type	Density (g/cm^3)	Tensile Strength (MPa)	Elongation (%)	Failure Strain	Moisture Regain	Avg. Dia. (d) (mm)	Length (l) (mm)	l/d
BF	1.3	780	3	2	60	0.16	10 20	63 125
JF	1.3	750	1.7	3	17	0.20	10 20	50 100

2.3. Mix Proportions of Quaternary-Blended Composites

Based upon the initial trial, OPC of 20% and MK of 30% were maintained constant for all the mixes. The percentage of WA content was varied from 5% to 25%. The RHA content balanced the remaining percentage of material. The binder/sand ratio was kept at 1:2 [41]. Accordingly, the binder materials are 334 kg/m^3, and the fine aggregate is 666 kg/m^3. The volume fraction of each fibre was maintained at 0.25%; hence, the total volume fraction of fibres was 0.5%. The water-to-binder ratio was maintained at 0.5 for all the mixes. Fifteen mixes were proposed for QBC, as presented in Table 3. The powdered materials, viz., OPC, MK, RHA, and WA, were dry-mixed for 1 min at moderate speed in a mixer and river sand was added to the mix [49]. The natural fibres were added slowly and evenly to the mixtures. Water was added at intervals and proportionately for about 3–4 min, and a uniform distribution of natural fibres was ensured in the mixture to avoid the balling effect of fibres. The experimental methodology is added in Figure 3.

Table 3. Mix proportions of quaternary-blended composites.

Mix ID	Length of Fibers (mm)	OPC (kg/m^3)	MK (kg/m^3)	RHA (kg/m^3)	WA (kg/m^3)	FA (kg/m^3)
MC1	-	66	101	150	17	666
MC2	-	66	101	134	33	666
MC3	-	66	101	117	50	666
MC4	-	66	101	101	66	666
MC5	-	66	101	84	83	666
M1L1	10	66	101	150	17	666
M2L1	10	66	101	134	33	666
M3L1	10	66	101	117	50	666
M4L1	10	66	101	101	66	666
M5L1	10	66	101	84	83	666
M1L2	20	66	101	150	17	666
M2L2	20	66	101	134	33	666
M3L2	20	66	101	117	50	666
M4L2	20	66	101	101	66	666
M5L2	20	66	101	84	83	666

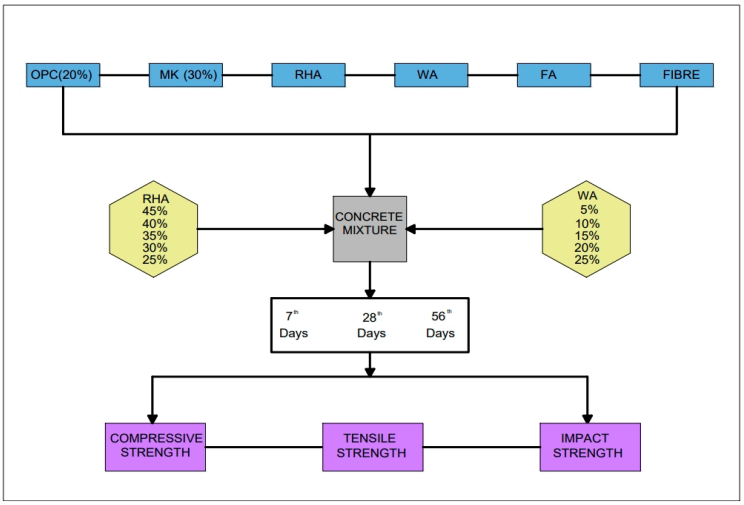

Figure 3. Experimental methodology.

2.4. Experimental Test Methods

Forty-five mortar cube specimens of 70.6 mm × 70.6 mm × 70.6 mm were tested for compressive strength [50]. For the split tensile strength [51], 45 cylindrical specimens (100 mm in diameter and 200 mm in height) were cast. A drop-weight hammer of an impact testing set-up is shown in Figure 3. The impact strength test of mortar specimens was carried out following ACI 544.2R—89 [52]. The specimens in disc form 150 mm in diameter with a thickness of 50 mm were cast for the impact strength test. The impact on the surface of the disc specimen was produced by dropping a hammer of 4.54 kg from a height of 457 mm, as presented in Figure 4. The hammer was dropped, and the number of blows essential to cause the first visible crack on the topmost surface of the disc specimen (N1) and the ultimate failure (N2) was recorded. At every crack level, the impact energy (IE) was computed by Equation (1).

$$\text{Impact Energy, IE} = \text{N}\cdot\text{m}\cdot\text{g}\cdot\text{h} \quad (1)$$

where N = number of blows at the crack formation; m = mass of the drop hammer in kg; g = acceleration due to gravity in m/s^2; h = drop height in mm. Three sample specimens in all the tests were performed at 7, 28, and 56 days. The scanning electron microscope (SEM) test was conducted to study the morphological characteristics of the selected mortar specimens.

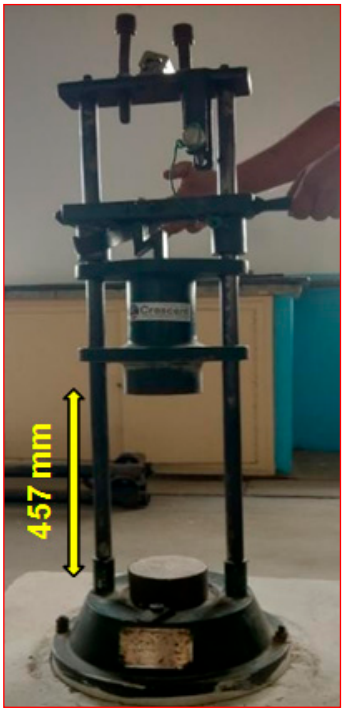

Figure 4. Impact strength test set-up.

2.5. Neural Network Modelling

In the present study, the "tool" in MATLAB was employed to process the data. An ANN model was developed by using these experimental values. The testing data were chosen as the subset of the training dataset (Appendix A) for improved accuracy and predictability of the ANN model [53]. This was randomly be selected from the total dataset. During ANN processing, the entire dataset was randomly be allocated into train–test–validation sets of 70–15–15%, respectively. For the prediction of compressive strength, tensile strength, and impact strength of QBC, the "Feed-Forward Back-Propagation" framework was used. A basic ANN model generally consists of input and output layers along with one hidden layer. The inputs were considered as the length of the fibre, RHA, WA, and

curing days. The target outputs were compressive strength, tensile strength, and impact strength of QBC. The ranges of input and output parameters for ANN modelling are shown in Table 4.

Table 4. Ranges of input and output parameters for ANN.

Input/Output	Parameters	Range
Input	Fibre length	0–20
	RHA	0–150
	WA	0–100
	Curing days	7–56
Output	Compressive strength	2.07–12.56
	Tensile strength	0.42–2.94
	Impact strength	977–3969

2.6. Training Methodology

The gradient descent momentum and adaptive learning rate (traingdx) were chosen as the training function with a "LOGSIG" as the transfer function. The number of epochs and validation checking were kept at 10,000 and 1×10^{-5} as a minimum gradient for more accuracy. During the training stage, the number of hidden layers and their neurons was altered to obtain the closest results to the experimental values so that the errors would be minimal. Since a simplified ANN model was chosen, only one hidden layer with various hidden neurons, such as 5, 7, 8, 9, and 10 [54,55], was performed. The performance of the ANN model in predicting compressive strength, tensile strength, and impact energy was evaluated using several error metrics, including the correlation coefficient (r), coefficient of determination (R^2), root mean squared error (RMSE), mean absolute error (MAE), and mean absolute percentage error (MAPE) [56–58]. The network architecture is given in Figure 5.

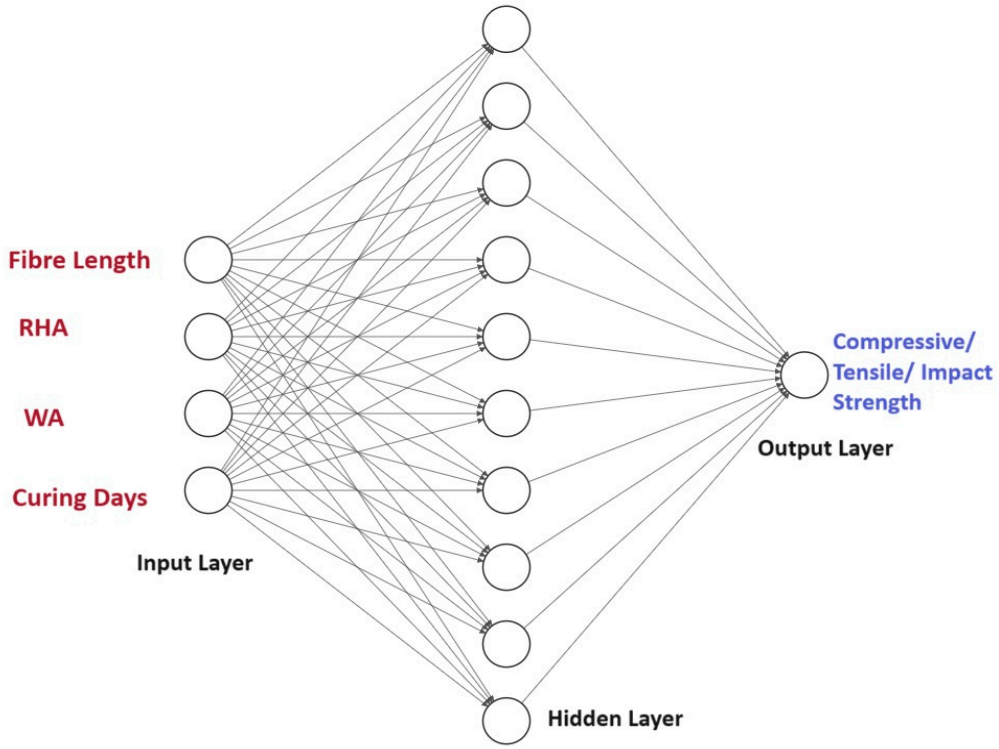

Figure 5. Network architecture.

3. Test Results and Discussions

3.1. Compressive Strength

The average compressive strength of various mixes for different curing days are presented in Figure 6. From the results obtained from 7 days of testing, M4L2 performed well in terms of strength, preceding the strength values of M4L1 due to the presence of fibre length, which arrests the cracks for a longer application of load. Lower strength was attained in MC1. The mixes M1L1 and M1L2 produced similar strength results of 2.34 N/mm^2. The results obtained from the control mixes were lower when compared to the mixes incorporated with fibres. Short fibres of 10 mm in length incorporated in the mixes resulted in lower strength than the 20 mm fibres. The mix M4L2 of 10.97 N/mm^2 performed well at 28 days of curing, whereas M1L2 resulted in lower strength results due to the incorporation of 45% rice husk ash. As the age of curing increases, the strength values increase, and a similar trend was observed in the earlier findings [20]. By observing the results, it was found that there is a gradual increase in strength with the replacement of wood ash ranging from 5% to 20%, after which there is a reduction in the strength values. While comparing the results of 56 days of testing, mix M4L2 performed well in terms of strength results, whereas MC5 resulted in a lower strength value. There is a percentage increase in strength of about 51.03% for mix M4L2 compared to control mix MC4. On comparing the results of 56 days of testing with 28 days, there is an increase in strength of 12.70%.

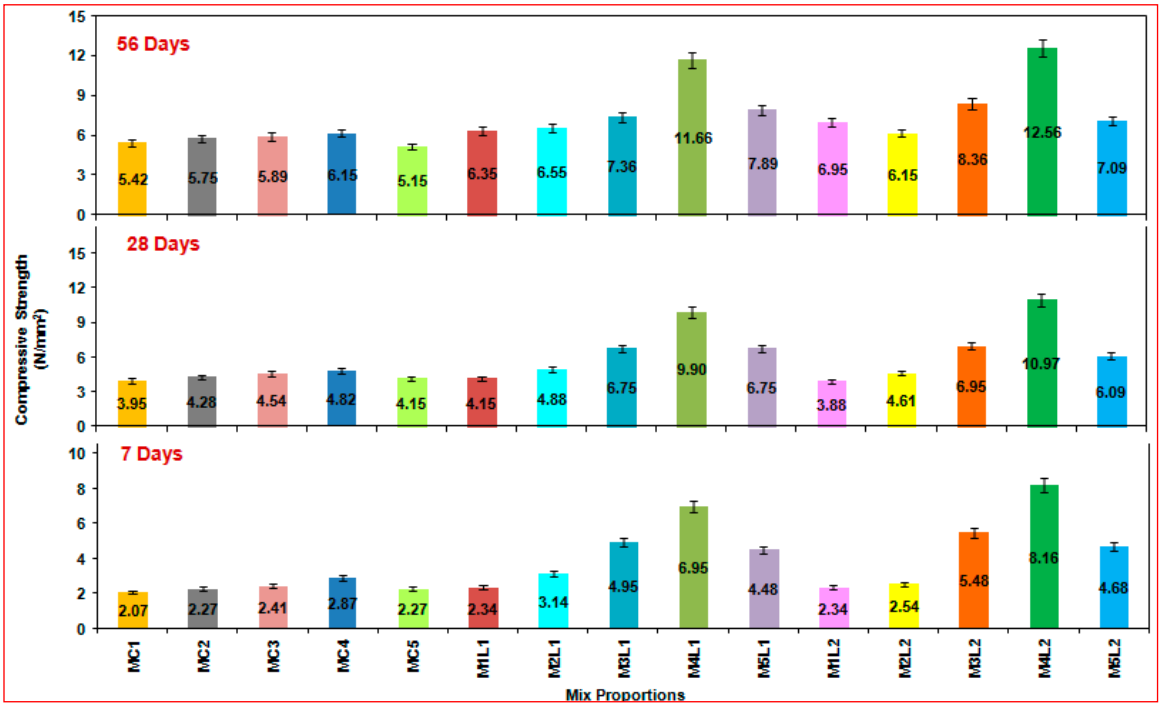

Figure 6. Results of compressive strength of QBC.

The failure patterns of cube specimens subjected to the compressive strength test are shown in Figure 7. The type of failure that occurred in the cube specimens of QBC is crushing failure. Upon observing the specimens during the test, the failure of control specimens was brittle and destructive, with a loud noise. In contrast, the failure pattern was found to be similar to that of the control specimen incorporated with a 10 mm length of fibres, which consumes a certain amount of energy and postpones the crack formation. However, specimen M4L2 consumes an enormous amount of energy and develops fine cracks at a later period, and the resulting failure pattern changes from brittle to quasi-ductile.

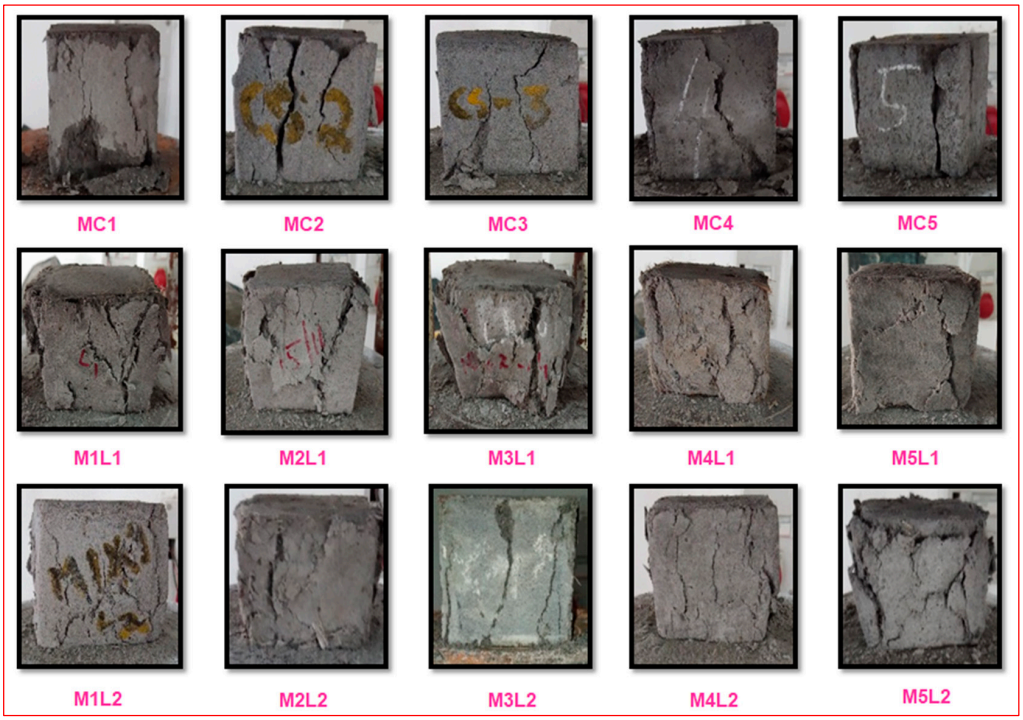

Figure 7. Typical failure patterns of cube specimens of QBC.

3.2. Splitting Tensile Strength

The average results of the split tensile strength for various ages of testing (7, 28, and 56 days) are depicted in Figure 8. At 7 days of testing, mix M4L2 produced a higher strength value, whereas M5L1 produced a lower strength value. Observing the results illustrates that there is a gradual increase in strength with the replacement of wood ash ranging from 5% to 20%, after which there is a reduction in the strength values. From the results obtained from 28 days of curing, the higher tensile strength was attained in M4L2. Mixes MC1 and MC2 produced similar strength results. When comparing the results of all mixes, the control mixes attained lower strength values. Observing the results, it was concluded that the increase in RHA content beyond 25% and WA content beyond 20% leads to lower strength values. A similar trend pattern of strength results was observed from the research work of Kanchan Mala et al. [59]. Similar strength results were observed in mixes MC4 and M2L2.

The highest strength value was achieved in M4L2 at 56 days of testing, whereas the lowest strength was obtained in MC3. There is an increase in the strength percentage of about 29.19% for mix M4L2 when compared to control mix MC4. The mixes M4L1 and M5L2 produced similar strength results. On comparing the results of 56 days of testing with 28 days, there was an increase in strength of 31.84%. The failure pattern of cylindrical specimens subjected to the spilt tensile strength test is shown in Figure 9. Failure of control specimens was accompanied by a huge noise separated into two halves due to brittle nature [60]. The failure mode of cylindrical specimens incorporated with a 10 mm length of fibres was similar to that of the control mixes, and there was a delay in the formation of cracks, which occurred due to the presence of fibres in the mix. The type of failure that occurred in M4L2 is a columnar fracture with lower noise in which the finer cracks were arrested by the presence of 20 mm fibres, and the crack formation was prolonged more when compared to the other mixes.

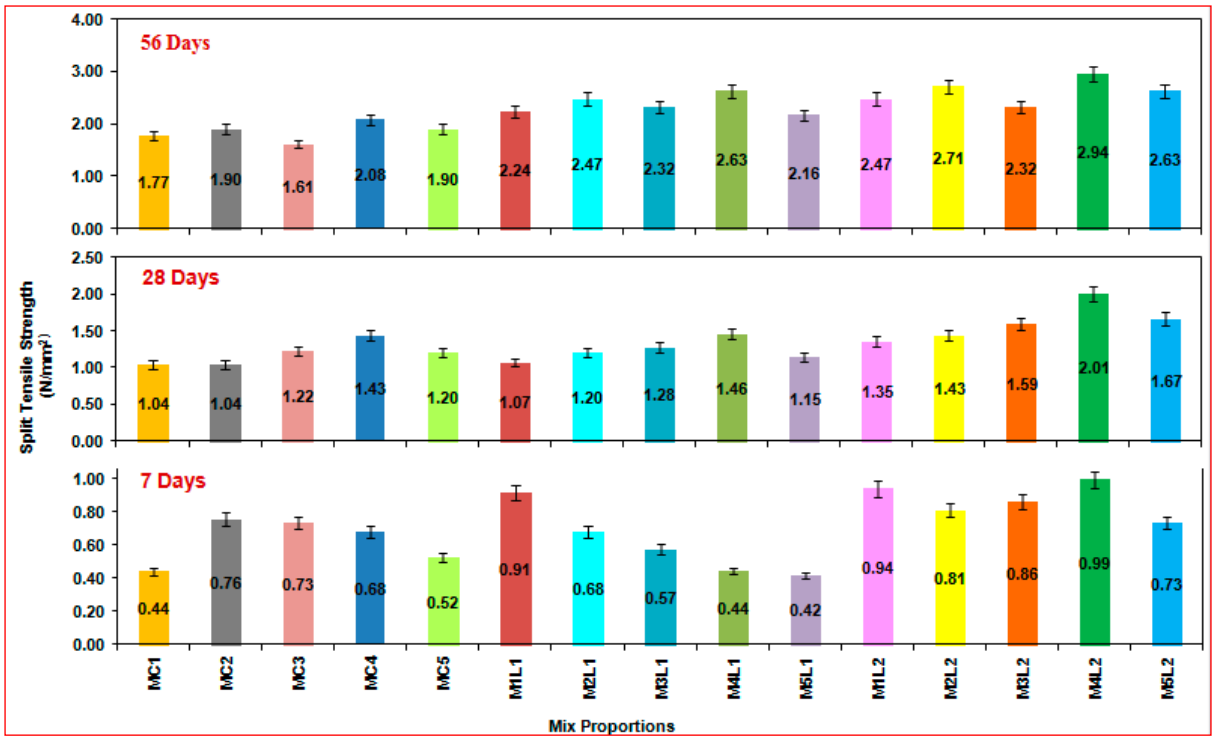

Figure 8. Results of split tensile strength of QBC.

Figure 9. Typical failure patterns of cylinder specimens of QBC.

3.3. Impact Strength

The results obtained from the impact strength test of QBC are illustrated in Table 5. The initial value denotes the number of blows required to make the first visible crack (N1), whereas the final value denotes the ultimate failure (N2) of the specimen. If the number of blows increases, it leads to an increase in the impact energy value. Figure 10 represents the impact energy values of QBC for different ages of curing obtained from the average results of the impact strength test. Observing the results obtained, control mixes suddenly failed, compared to those incorporated with fibres of various lengths. From the results obtained at 7 days of curing, the mix M5L1 withstands a larger number of blows due to the presence of fibres of length 10 mm when compared to all the other mixes; hence, the impact energy produced is greater. The lesser impact energy values were obtained in MC1. Comparing the results of M5L1 with control mix MC5, we see an increase in its impact energy value of about 17.37%. The results obtained at 28 days of curing showed that mix M5L1 produced a higher impact energy value than the other mixes, whereas mix MC1 produced a lower value. Hence, the impact energy value obtained at 28 days is slightly higher than the values obtained in the 7 days of curing.

Table 5. Number of blows at initial and final stage of impact strength test of QBC.

Mix ID	Number of Blows					
	7 Days		28 Days		56 Days	
	Initial Stage (N1)	Final Stage (N2)	Initial Stage (N1)	Final Stage (N2)	Initial Stage (N1)	Final Stage (N2)
MC1	20	48	25	53	38	71
MC2	26	57	31	63	40	73
MC3	33	82	39	82	47	94
MC4	31	74	36	81	30	80
MC5	38	100	43	107	53	124
M1L1	59	123	66	128	72	159
M2L1	54	112	58	115	66	168
M3L1	67	115	73	123	81	186
M4L1	60	108	65	110	75	173
M5L1	74	121	80	126	91	195
M1L2	55	109	58	113	67	154
M2L2	52	105	55	107	58	163
M3L2	60	111	63	113	75	175
M4L2	52	96	57	100	69	179
M5L2	70	116	74	118	90	182

Comparing the results of M5L1 with control mix MC5, there is an increase in its impact energy value of about 15.08%. From the results obtained from 56 days of curing, it was concluded that due to the presence of wood ash in the mix, its impact energy value increases as the age of curing increases, and a similar trend pattern was observed [61]. M5L1 obtained a higher energy value because it had withstood a greater number of blows compared to the other mixes. The results obtained from mix MC1 produced the lowest impact value of all the mixes. There is a percentage increase in energy value of about 36.40% for mix M5L1 when compared to control mix MC5 at 56 days of testing. On comparing the results of 56 days of testing with 28 days, there was a percentage increase in its energy value of about 35.37%.

The failure patterns of specimens subjected to the impact strength test are shown in Figure 11. Figure 12 depicts the formation and propagation of cracks at (a) the first crack stage, (b) the post-cracking stage, and (c) the failure stage of QBC disc specimens. Based on the results obtained from this test, it was found that the control mix specimens had been broken down and shattered into small multiple fragments, which had a minimum blow number of 50. Whereas the specimens incorporated with the fibres in the mix had withstood a larger number of blows, having a minimum value of 110 blows for mixes

having a 10 mm fibre length and 90 blows for mixes having a 20 mm fibre length. Hence, fibres of 10 mm in length were found to be more effective than those of 20 mm in length. There was a gradual increase in impact energy value by using WA up to 15% and RHA up to 35%, beyond which there was a slight decrease in the impact energy value.

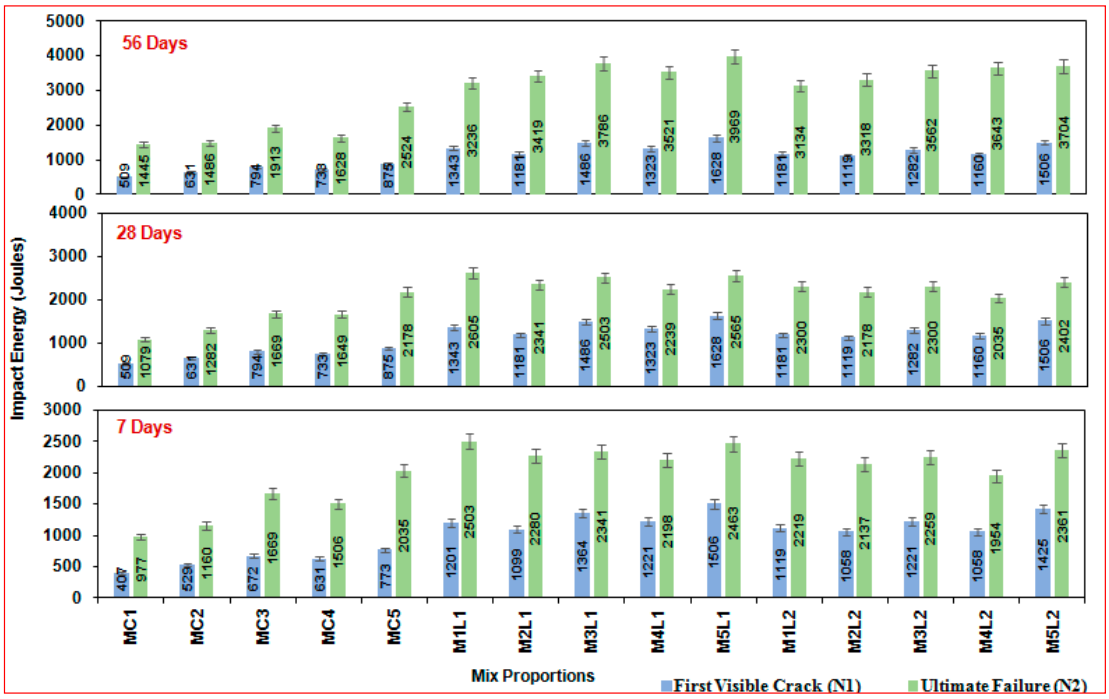

Figure 10. Results of impact strength test of QBC.

Figure 11. Typical failure patterns of disc specimens of QBC.

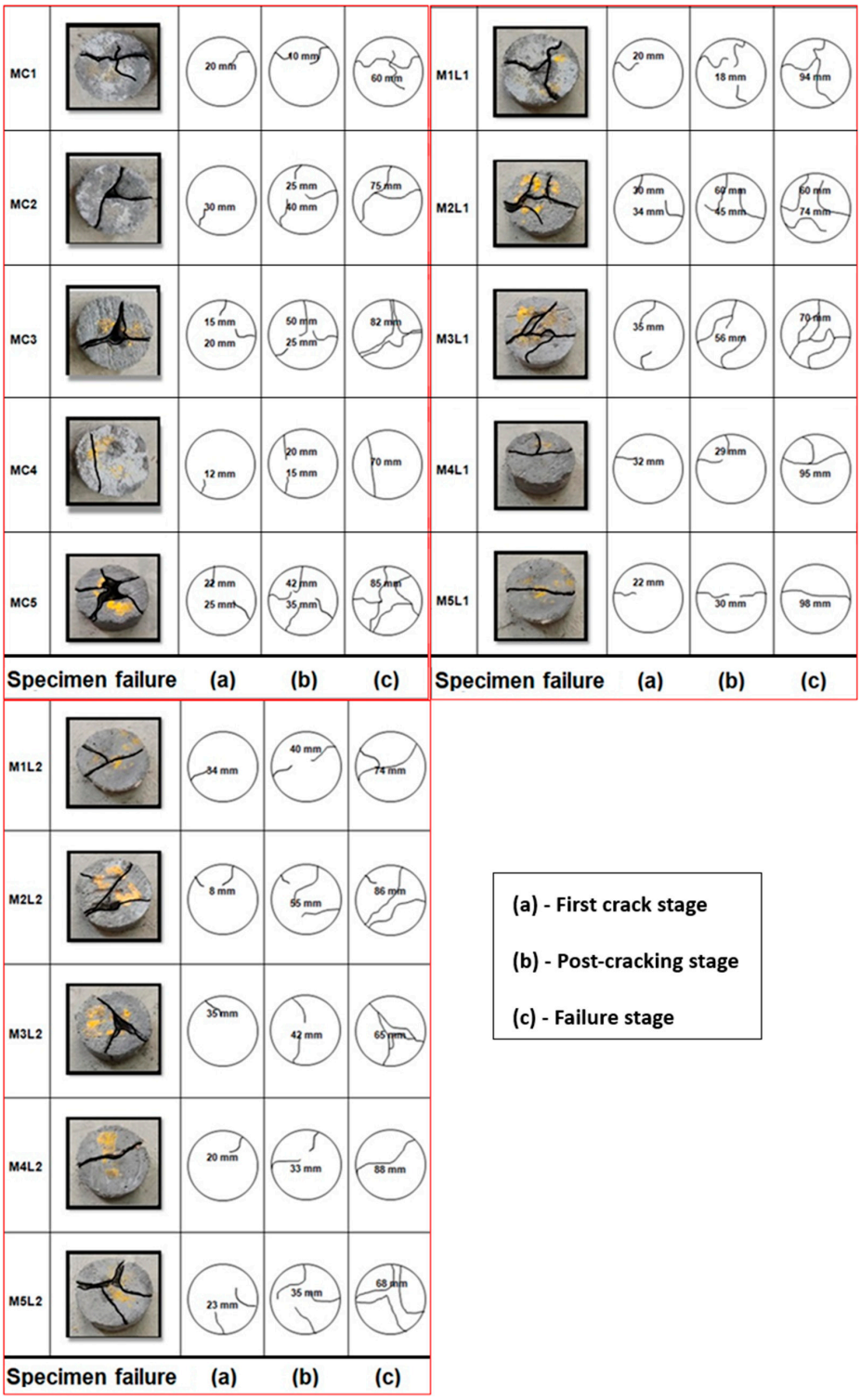

Figure 12. Formation and propagation of cracks in QBC disc specimens.

3.4. Microstructural Study

The SEM analysis was carried out for the control mix (MC4) and mix M4L2, presented in Figures 13 and 14, respectively. One of the interesting features of the microstructural study reveals that the fine strands of hybrid fibres were extended longitudinally among all composites. SEM analysis was conducted qualitatively and quantitatively to assess the microstructure of the cement matrix and the chemical composition of the C–S–H (calcium silica hydrate) gel present in the QBC. It was observed that there is a huge difference in

the surface texture of MC4 and M4L2. Observing the SEM images, the control mix shows the maximum surface of the sample is covered by the unhydrated portions. In contrast, the unhydrated portions of cement were found to be lesser in the case of M4L2. Larger crack formation was observed in the control mix. In contrast, the formation of cracks was resisted by the presence of hybrid natural fibres in the quaternary-blended mix of M4L2. Larger voids were present in MC4. The microstructure of M4L2 resulted in the denser composition of the matrix with less porosity, which was attributed to the synergic action of QBC. Supplementary cementitious materials such as metakaolin (30%), rice husk ash (30%), and wood ash (20%) are composed of finer particles that, when replaced by cement (20%), tend to occupy the spaces of voids, thereby reducing the formation of pores, which results in dense matrix formation. Hence, microcrack formation was greatly reduced and contact with fine aggregates was improved. In addition, C–S–H gel formation was observed, which is one of the important elements present in QBC, as it improves the cementitious/binding properties of the end product, hence resulting in increased strength. Due to the presence of fibres, even the minute cracks had been arrested, resulting in higher strength. The use of SCM, in addition to cement, significantly improves the morphology and enhances the microstructural aspects of quaternary-blended composites.

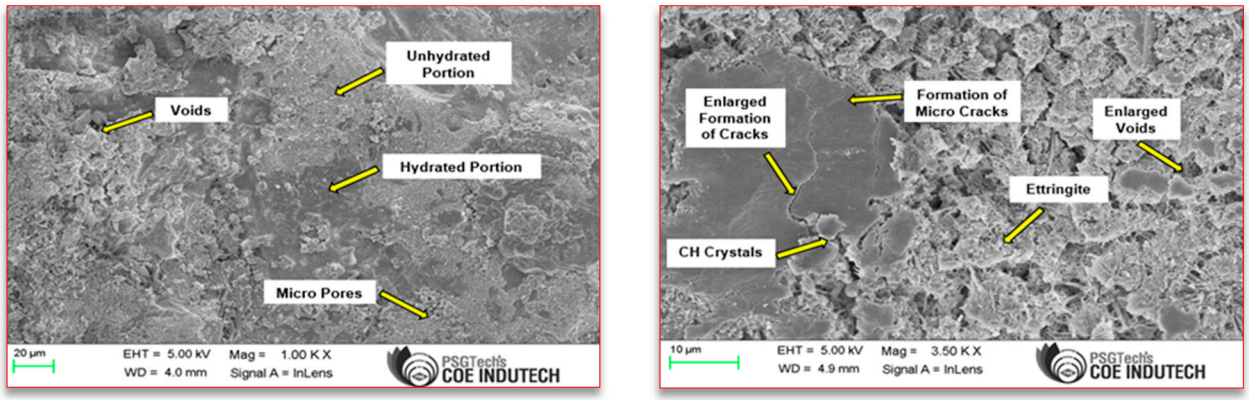

(**a**) (**b**)

Figure 13. SEM image of MC4: (**a**) resolution of 20 µm; (**b**) resolution of 10 µm.

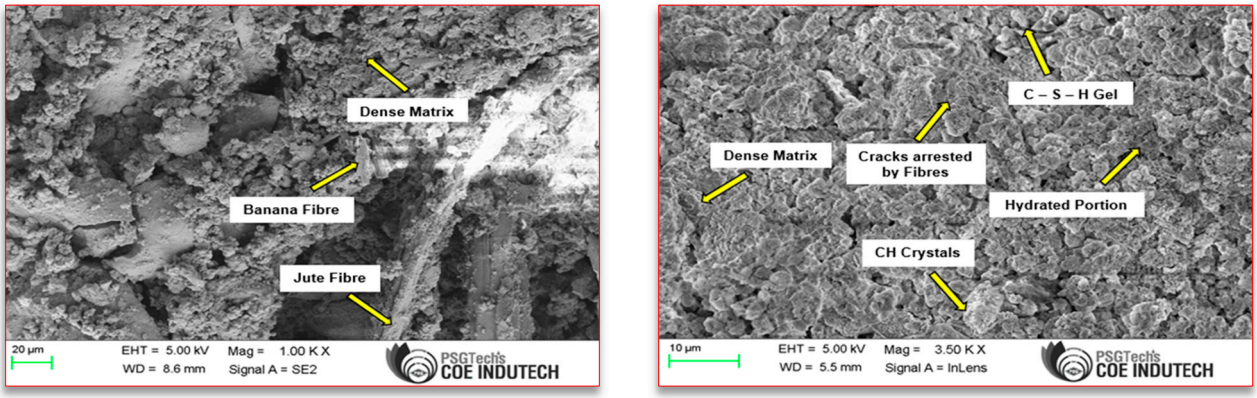

(**a**) (**b**)

Figure 14. SEM image of M4L2: (**a**) resolution of 20 µm; (**b**) resolution of 10 µm.

4. Proposed Expressions for Synergic Action of Binder Materials

The present study is focused on obtaining the efficiency factor for various SCMs, including metakaolin, rice husk ash, and wood ash, based upon which compressive strength can be predicted. To obtain the efficiency factor of QBC, an equation was developed based

on the findings of Bolomey's equation to predict the results of compressive strength [62], as given in Equation (2).

$$f_c(days) = A_1\left(\frac{C}{W}\right) + A_2 \tag{2}$$

By considering the individual effect of SCM, Bolomey's equation is modified as given below in Equation (3). The equation to obtain the efficiency factor of individual admixture k_{MA} is given in Equation (4).

$$f_c(days) = A_1\left[\frac{(C + k_{MA}\ P_{MA}\ )}{W}\right] + A_2 \tag{3}$$

$$k_{MA} = \left(\frac{1}{P_{MA}}\right)\left[-C + W\left(\frac{f_c\ - A_2}{A_1}\right)\right] \tag{4}$$

Since the efficiency factor of individual admixture can be obtained from the above equation, it is essential to compute the combined effect of SCM, which is expressed in terms of k_{TB} and can be calculated using Equation (5). The final efficiency factor (k'_{MA}) is calculated by using Equation (6).

$$k_{TB} = \{W[(f_c - A_2)/A_1] - C\}/(k_{MA}P_{MA}) \tag{5}$$

$$k'_{MA} = k_{TB}\ k_{MA} \tag{6}$$

where k'_{MA} = final efficiency factor.

An equation was developed to predict the strength of the binary mix, as given in Equation (6). Similarly, Equation (7) is modified to compute the strength of ternary and quaternary mixes and is given in Equations (8) and (9).

$$f_c(days) = A_1\left[\frac{C}{W} + k_{TB}\ (k_{MA}\ P_{MA})/W\right] + A_2 \tag{7}$$

$$f_c(days) = A_1\left[\frac{C}{W} + k_{TB}\ (k_{MA1}\ P_{MA1} + k_{MA2}\ P_{MA2})/W\right] + A_2 \tag{8}$$

$$f_c(days) = A_1\left[\frac{C}{W} + k_{TB}\ (k_{MA1}\ P_{MA1} + k_{MA2}\ P_{MA2} + k_{MA3}\ P_{MA3}\ )/W\right] + A_2 \tag{9}$$

where k'_{MA} = final efficiency factor; f_c = predicted compressive strength in N/mm^2; A_1 and A_2 = coefficients for dissimilar ages of testing; C = amount of cement (kg/m^3); W = amount of water (kg/m^3); k_{MA} = efficiency factor; P_{MA} = quantity of admixture (kg/m^3); k_{TB} = synergic factor of admixtures. In this study, Equation (9) was modified to predict the compressive strength of QBC with coefficients such as α_{MA}, α_{MK}, α_{RHA}, and α_{WA}, as shown in Equation (10)

$$f_c(days) = X_1\left[\frac{C}{W} + \alpha_{MA}\left(\alpha_{MK}\ P_{MK} + \alpha_{RHA}\ P_{RHA} + \alpha_{WA}\ P_{WA} + V_{f1} + V_{f2}\right)/W\right] + X_2 \tag{10}$$

where X_1 and X_2 = coefficients for different ages of curing; α_{MA} = synergic factor of mineral admixtures; α_{MK} = factor of efficiency for metakaolin; α_{RHA} = factor of efficiency for rice husk ash; α_{WA} = factor of efficiency for wood ash; P_{MK} = amount of metakaolin (kg/m^3); P_{RHA}= amount of rice husk ash (kg/m^3); P_{WA} = amount of wood ash (kg/m^3); V_{f1} = volume fraction 1 (0.25%); V_{f2} = volume fraction 2 (0.25%).

The following steps were adopted to obtain the synergistic action of QBC:

Step 1: The compressive strength results of control mixtures by maintaining a constant w/b ratio of 0.5 were fed into Origin Pro software (2022) as input.

Step 2: Equation (10) was used to compute the coefficients X_1 and X_2 at the ages of 7, 28, and 56 days.

Step 3: Then, α_{MA} was computed for various mixes at different curing ages.

Table 6 lists the constants X_1 and X_2 of various mixes for different ages of testing. Table 7 lists the synergic factor and analogous coefficients of SCM for different ages of testing.

Table 6. Constants X_1 and X_2 for different ages of testing.

Mix ID	Age of Testing	X_1	X_2
MC1	7	−5.20	2.60
	28	5.22	−2.61
	56	−2.60	1.30
MC2	7	−5.22	2.61
	28	−5.20	2.60
	56	5.22	−2.61
MC3	7	−0.53	2.67
	28	5.20	−2.60
	56	1.04	−5.20
MC4	7	−4.99	2.49
	28	0	4.81
	56	5.22	−2.61
MC5	7	−5.22	2.61
	28	−1.04	5.22
	56	−1.04	5.22
M1L1	7	5.22	−2.61
	28	5.22	−2.61
	56	5.22	−2.61
M2L1	7	−1.04	5.22
	28	−5.20	2.60
	56	−1.04	5.20
M3L1	7	−1.04	5.20
	28	−1.04	5.22
	56	−1.04	5.22
M4L1	7	−1.04	5.20
	28	−5.22	2.61
	56	1.65	−8.26
M5L1	7	−2.08	1.04
	28	−1.04	5.22
	56	−5.22	2.61
M1L2	7	5.22	−2.61
	28	−5.22	2.61
	56	−1.04	5.20
M2L2	7	5.22	−2.61
	28	0	4.61
	56	5.22	−2.61
M3L2	7	−5.22	2.61
	28	−1.04	5.20
	56	−1.04	5.22
M4L2	7	−1.04	5.20
	28	−1.04	5.22
	56	5.20	−2.60
M5L2	7	−5.22	2.61
	28	−5.22	2.61
	56	−5.22	2.61

Table 7. Synergic factor and analogous coefficients of SCM.

Mix ID	Age of Testing	α_{MA}	α_{MK}	α_{RHA}	α_{WA}
MC1	7	0.042	0.296	0.199	1.760
	28	−0.091	1.988	1.338	11.813
	56	0.041	−2.413	−1.624	−14.337
MC2	7	0.034	0.233	0.176	0.715
	28	0.094	−0.418	−0.315	−1.279
	56	−0.090	2.570	1.937	7.868
MC3	7	0.003	2.068	1.785	4.177
	28	−0.090	2.186	1.887	4.416
	56	−0.016	17.311	14.944	34.970
MC4	7	−4.306	0.002	0.002	0.003
	28	0	0	0	0
	56	−0.089	2.700	2.700	4.131
MC5	7	0.034	0.233	0.281	0.284
	28	0.011	2.366	2.845	2.879
	56	0.002	0.743	0.893	0.904
M1L1	7	−0.093	1.470	0.990	8.739
	28	−0.091	2.053	1.382	12.198
	56	−0.089	2.764	1.861	16.426
M2L1	7	0.013	3.989	3.007	12.211
	28	0.088	−0.612	−0.462	−1.876
	56	0.021	−1.561	−1.176	−4.778
M3L1	7	0.006	1.036	0.894	2.093
	28	0.020	−1.854	−1.600	−3.745
	56	0.018	−2.828	−2.441	−5.713
M4L1	7	0.019	−2.210	−2.210	−3.382
	28	0.077	−2.224	−2.224	−3.404
	56	−0.026	19.925	19.925	30.491
M5L1	7	0.034	−2.469	−2.969	−3.005
	28	0.020	−1.854	−2.229	−2.256
	56	0.079	−1.577	−1.896	−1.919
M1L2	7	−0.093	1.470	0.990	8.739
	28	0.105	−0.283	−0.191	−1.685
	56	0.019	−2.210	−1.488	−13.132
M2L2	7	−0.092	1.535	1.157	4.700
	28	0	0	0	0
	56	−0.089	2.700	2.035	8.263
M3L2	7	0.084	−0.801	−0.691	−1.618
	28	0.019	−2.210	−1.908	−4.465
	56	0.017	−4.451	−3.843	−8.992
M4L2	7	0.017	−4.158	−4.158	−6.364
	28	0.016	−8.672	−8.672	−13.272
	56	−0.087	4.782	4.782	7.318
M5L2	7	0.090	−0.542	−0.652	−0.660
	28	0.082	−0.995	−1.196	−1.2117
	56	0.080	−1.318	−1.585	−1.604

The constants X_1 and X_2 from Table 6 and the synergic factor and their coefficients from Table 7 were substituted in the equations corresponding to the ages of curing. The compressive strength results were obtained by solving those equations. The results obtained from the experimental compressive strength values and the predicted compressive strength values and their percentage differences are given in Table 8. There was a significant

difference in the strength values compared to the value obtained from the experimental work. At 7 days of testing, the predicted value of M4L2 was lower when compared to the experimental value, whose percentage difference was 7.04. The highest percentage difference was attained at M5L1, and the lowest percentage difference was attained at MC2. While comparing the strength results for 28 days of curing, the predicted value of M4L2 was higher, and the percentage difference was 8.96. The highest percentage difference was attained at M1L2, and the lowest percentage difference was attained at M3L1. The predicted strength value obtained at 56 days of curing is significant to that of the experimental value of compressive strength. The percentage difference for M4L2 was found to be 4.06. The lowest percentage difference was attained at 1.62, whereas the highest percentage difference was attained at MC3.

Table 8. Experimental vs predicted values of compression strength test.

MIX ID	Experimental Compressive Strength (N/mm^2)			Predicted Compressive Strength (N/mm^2)			Difference (%)		
	7 Days	28 Days	56 Days	7 Days	28 Days	56 Days	7 Days	28 Days	56 Days
MC1	2.073	3.945	5.416	2.472	4.102	5.163	17.55	3.90	4.78
MC2	2.273	4.280	5.751	2.325	4.956	6.050	2.26	14.63	5.06
MC3	2.407	4.543	5.885	2.524	4.907	5.185	4.74	7.70	12.64
MC4	2.872	4.815	6.152	2.667	4.356	6.652	7.40	10.00	7.81
MC5	2.273	4.146	5.149	2.524	3.908	5.546	10.46	5.91	7.42
M1L1	2.340	4.146	6.353	2.981	4.606	6.950	24.09	10.51	8.97
M2L1	3.143	4.882	6.553	4.121	4.205	6.015	26.92	14.90	8.56
M3L1	4.948	6.754	7.356	3.946	6.903	7.053	22.53	2.18	4.20
M4L1	6.954	9.897	11.661	5.279	9.108	11.473	27.38	8.30	1.62
M5L1	4.480	6.754	7.891	3.350	6.237	7.292	28.86	7.95	7.89
M1L2	2.340	3.878	6.954	2.145	3.102	6.154	8.69	22.23	12.20
M2L2	2.541	4.614	6.152	2.068	4.011	6.869	20.52	13.98	11.01
M3L2	5.483	6.954	8.359	4.954	6.249	8.157	10.13	10.67	2.44
M4L2	8.158	10.967	12.563	7.603	10.026	12.062	7.04	8.96	4.06
M5L2	4.681	6.085	7.088	5.165	7.010	7.485	9.83	14.12	5.44

5. Performance Evaluation of Strength Predictions of QCB from ANN Modelling

It is noted that the ANN models [4:5:1], [4:10:1], and [4:8:1] (indicated as 4 inputs; 1 hidden layer with 5,10, and 8 neurons; and 1 output) were the best possible outcomes for compressive strength, tensile strength, and impact strength, respectively. The performance in terms of best-suited validation, training stage, and regression results for the ANN models [4:5:1], [4:10:1], and [4:8:1] is presented in Figure 15. A comparison of observed and modelled values for the strength characteristics of QBC of 7, 28, and 56 days are presented in Figure 16.

The overall performance of the model for various strength parameters of QBC was evaluated through statistical error parameters, summarised in Table 9. In all cases, R values more than 0.9 signify a strong correlation between the observed and modelled results. This demonstrates that the generated ANN structure, trained using experimental results, truly predicted the target values. It can be inferred that the ANN models [4:5:1], [4:10:1], and [4:8:1] could be employed for predicting the compressive strength, tensile strength, and impact energy of quaternary-blended composites.

Table 9. Overall statistical parameters of ANN models for strength parameters of QBC.

Parameters	Compressive Strength			Tensile Strength			Impact Energy		
	7 Days	28 Days	56 Days	7 Days	28 Days	56 Days	7 Days	28 Days	56 Days
R	0.990	0.997	0.963	0.951	0.965	0.951	0.994	0.997	0.995
R^2	0.981	0.995	0.927	0.903	0.932	0.904	0.989	0.995	0.991
RMSE	0.255	0.150	0.562	0.080	0.092	0.146	54.750	31.280	94.230
MAE	0.152	0.118	0.410	0.069	0.065	0.112	34.215	23.810	46.860
MAPE	4.250	2.236	5.551	11.380	4.600	4.990	2.390	1.201	1.530

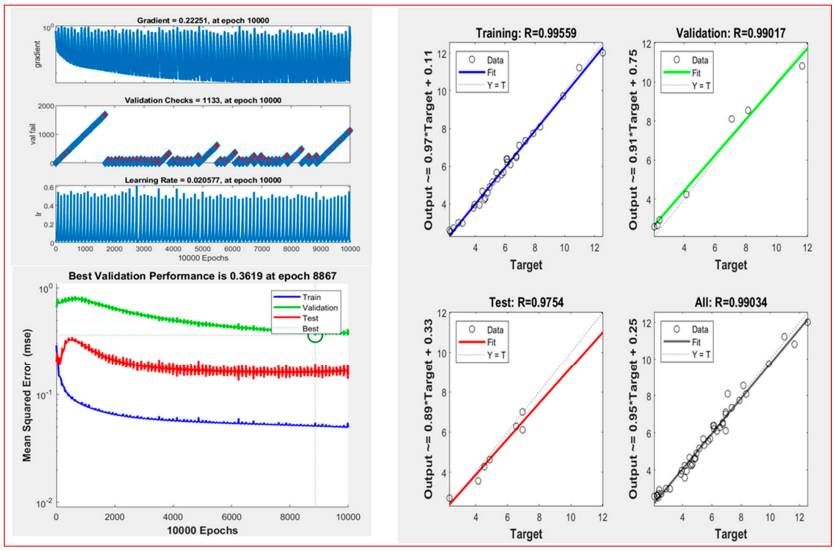

(**a**)

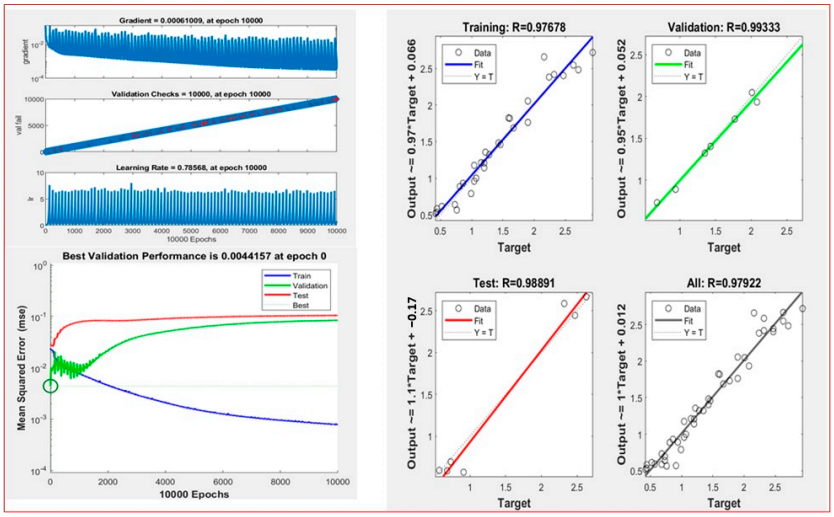

(**b**)

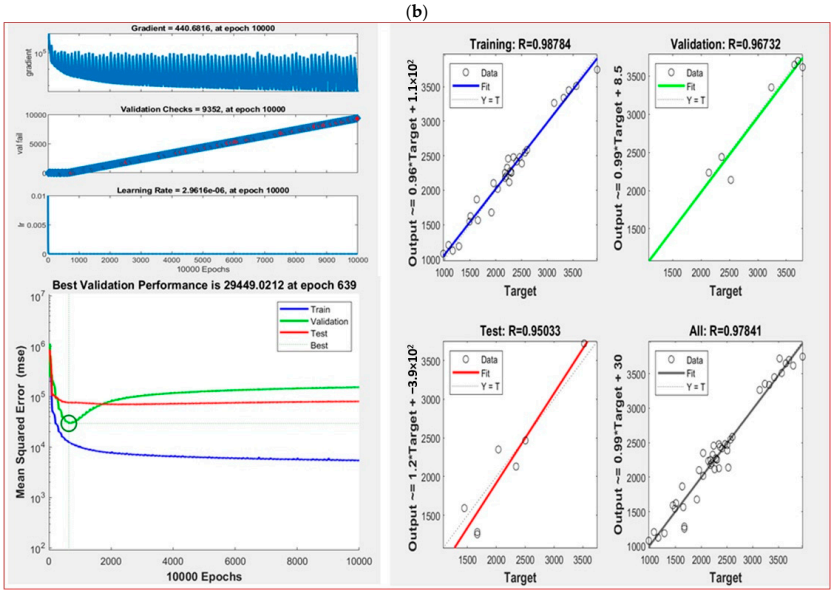

(**c**)

Figure 15. Best-suited validation, training stage, and regression results for the ANN models: (**a**) [4:5:1]; (**b**) [4:10:1]; (**c**) [4:8:1] for compressive strength, tensile, strength, and impact energy of QBC.

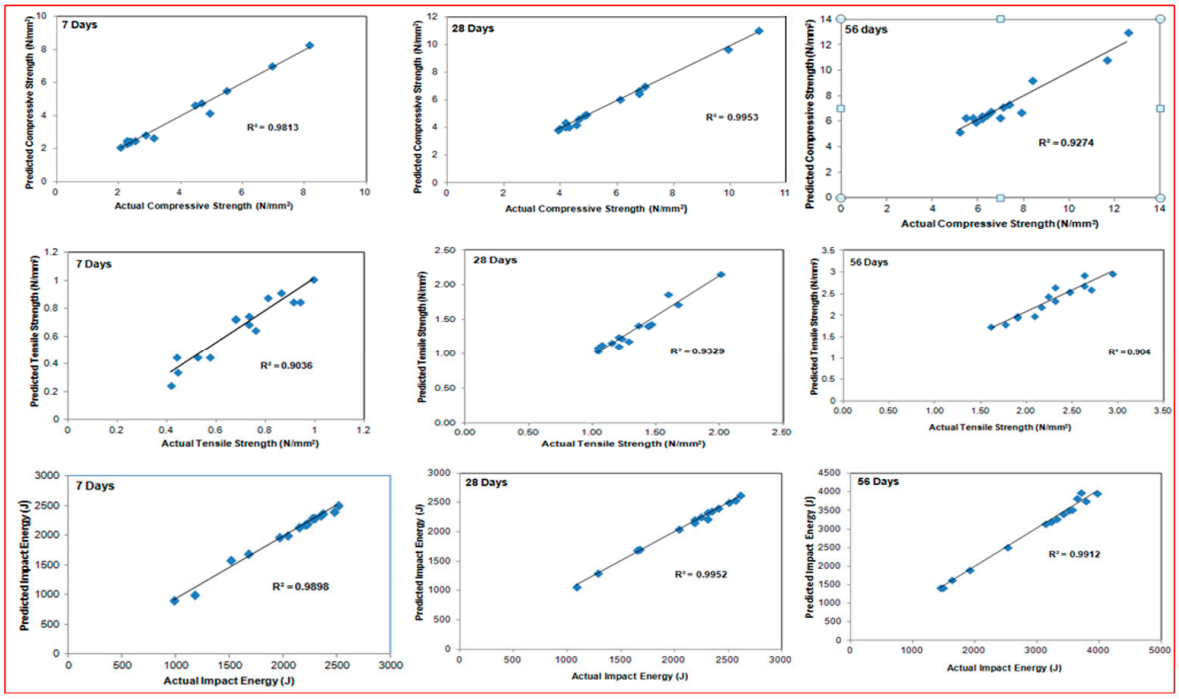

Figure 16. Comparison of observed and modelled values for the strength characteristics of QBC at 7, 28, and 56 days.

6. Conclusions

This work aimed to evaluate the viability of using different agro-industrial waste pozzolanic materials, including ordinary Portland cement, metakaolin, rice husk ash, and wood ash, in the production of sustainable concrete. The hardened properties of these materials were obtained and then validated using scanning electron microscopy (SEM) and artificial neural networks (ANNs). Fifteen distinct ratios of pozzolanic ingredients, substituting varying percentages of cement, were included in the concrete. Several mechanical and durability tests were conducted, including compressive strength, split tensile strength, and impact strength. Furthermore, artificial neural networks (ANNs) were used in machine learning to improve the mix design. Below are a few key findings derived from the following research:

1. The highest compressive strength value was attained at M4L2, which was incorporated with fibres of 20 mm in length. The maximum strength attained at 56 days of testing was found to be 12.563 N/mm^2. On comparing the results of 56 days of testing with 28 days, there was an increase in strength of 12.70%. The increase in strength was about 51.03% for mix M4L2 compared to control mix MC4 at 56 days of testing.
2. Similarly, mix M4L2 produced a higher strength of about 2.942 N/mm^2 for the tensile strength. On comparing the results of 56 days of testing with 28 days, there was an increase in strength of 31.84%. There was an increase in strength of about 29.19% for mix M4L2 when compared to control mix MC4 at 56 days of testing.
3. The mix M5L1 produced higher impact energy among all the mixes. An increase in energy value of 35.37% was observed. Small strands of fibres with a length of 10 mm withstand a higher number of impact blows than the 20 mm length of fibres. There was an increase in energy value of about 36.40% for mix M5L1 when compared to control mix MC5 at 56 days of testing.
4. On observing the microstructural characteristics in MC4, larger cracks were developed, and larger voids were present. Meanwhile, characteristics of M4L2 were due to the proper cohesion of particles observed with a denser matrix. Only a few microvoids were present in M4L2. Due to the presence of hybrid fibres in the mix, most cracks

were arrested. Hence, adding metakaolin to the mix improves the binding properties and enhances the microstructure in QBC.

5. The efficiency factor showed a significant difference, and the strength values showed a synergic effect compared to the value obtained from the experimental work.
6. The ANN model used in this study to predict the compressive strength, tensile strength, and impact strength characteristics of QBC was found to be precise and agree well with the test results. ANN models [4:5:1], [4:10:1], and [4:8:1] were the best possible outcomes for compressive strength, tensile strength, and impact strength, respectively.

7. Scope for Future Work

The present investigation was limited in analysing the following mechanical parameters: compressive strength, split tensile strength, and impact strength, 56 days. Determining the elastic modulus and longitudinal behaviour of quaternary-blended specimens is necessary, as well the mechanical characteristics and rate of strength increase over 365 days. The use of artificial intelligence models can achieve further optimisation of quaternary-mixed concrete. Implementing such ANN models decreases the number of trials in the approach and leads to the development of more precise predictive models. This is because a greater quantity of data available significantly enhances the training phase of predictive models. This enables researchers to implement more accurate prediction models using diverse computational approaches, including response surface methodology, gene expression programming, and other optimisation techniques.

Author Contributions: Conceptualisation, P.C., M.R.N.A. and R.J.; methodology, R.J., G.P., V.S.K. and P.C.; software, M.R.N.A., P.C., R.J. and G.P.; validation, M.R.N.A., P.C. and V.S.K.; formal analysis, P.C., R.J. and G.P.; investigation, P.C. and M.R.N.A.; resources, M.R.N.A. and P.C.; data curation, P.C. and V.S.K.; writing—original draft preparation, P.C., M.R.N.A. and R.J.; writing—review and editing, G.P. and V.S.K.; supervision, R.J. and G.P.; project administration, V.S.K. and P.C. All authors have read and agreed to the published version of the manuscript.

Funding: This research received no external funding.

Data Availability Statement: The datasets generated during and/or analysed during the current study are available from the corresponding author upon reasonable request.

Conflicts of Interest: The authors declare no conflicts of interest.

Appendix A

Fibre Length (mm)	Cement (kg/m^3)	Metakaolin (kg/m^3)	Rice Husk Ash (kg/m^3)	Wood Ash (kg/m^3)	Fine Aggregate (kg/m^3)	Curing (Days)	Compressive Strength (N/mm^2)	Tensile Strength (N/mm^2)	Impact Strength (N/mm^2)
0	66	101	150	17	666	7	2.07	0.44	977
0	66	101	134	33	666	7	2.27	0.76	1160
0	66	101	117	50	666	7	2.41	0.73	1669
0	66	101	101	66	666	7	2.87	0.68	1506
0	66	101	84	83	666	7	2.27	0.52	2035
10	66	101	150	17	666	7	2.34	0.91	2503
10	66	101	134	33	666	7	3.14	0.68	2280
10	66	101	117	50	666	7	4.95	0.57	2341
10	66	101	101	66	666	7	6.95	0.44	2198
10	66	101	84	83	666	7	4.48	0.42	2463
20	66	101	150	17	666	7	2.34	0.94	2219
20	66	101	134	33	666	7	2.54	0.81	2137
20	66	101	117	50	666	7	5.48	0.86	2259
20	66	101	101	66	666	7	8.16	0.99	1954
20	66	101	84	83	666	7	4.68	0.73	2361

Fibre Length (mm)	Cement (kg/m^3)	Metakaolin (kg/m^3)	Rice Husk Ash (kg/m^3)	Wood Ash (kg/m^3)	Fine Aggregate (kg/m^3)	Curing (Days)	Compressive Strength (N/mm^2)	Tensile Strength (N/mm^2)	Impact Strength (N/mm^2)
0	66	101	150	17	666	7	2.07	0.44	977
0	66	101	134	33	666	7	2.27	0.76	1160
0	66	101	117	50	666	7	2.41	0.73	1669
0	66	101	101	66	666	7	2.87	0.68	1506
0	66	101	84	83	666	7	2.27	0.52	2035
10	66	101	150	17	666	7	2.34	0.91	2503
10	66	101	134	33	666	7	3.14	0.68	2280
10	66	101	117	50	666	7	4.95	0.57	2341
10	66	101	101	66	666	7	6.95	0.44	2198
10	66	101	84	83	666	7	4.48	0.42	2463
20	66	101	150	17	666	7	2.34	0.94	2219
20	66	101	134	33	666	7	2.54	0.81	2137
20	66	101	117	50	666	7	5.48	0.86	2259
20	66	101	101	66	666	7	8.16	0.99	1954
20	66	101	84	83	666	7	4.68	0.73	2361
0	66	101	150	17	666	28	3.95	1.04	1079
0	66	101	134	33	666	28	4.28	1.04	1282
0	66	101	117	50	666	28	4.54	1.22	1669
0	66	101	101	66	666	28	4.82	1.43	1649
0	66	101	84	83	666	28	4.15	1.2	2178
10	66	101	150	17	666	28	4.15	1.07	2605
10	66	101	134	33	666	28	4.88	1.2	2341
10	66	101	117	50	666	28	6.75	1.28	2503
10	66	101	101	66	666	28	9.90	1.46	2239
10	66	101	84	83	666	28	6.75	1.15	2565
20	66	101	150	17	666	28	3.88	1.35	2300
20	66	101	134	33	666	28	4.61	1.43	2178
20	66	101	117	50	666	28	6.95	1.59	2300
20	66	101	101	66	666	28	10.97	2.01	2035
20	66	101	84	83	666	28	6.09	1.67	2402
0	66	101	150	17	666	56	5.42	1.77	1445
0	66	101	134	33	666	56	5.75	1.9	1486
0	66	101	117	50	666	56	5.89	1.61	1913
0	66	101	101	66	666	56	6.15	2.08	1628
0	66	101	84	83	666	56	5.15	1.9	2524
10	66	101	150	17	666	56	6.35	2.24	3236
10	66	101	134	33	666	56	6.55	2.47	3419
10	66	101	117	50	666	56	7.36	2.32	3786
10	66	101	101	66	666	56	11.66	2.63	3521
10	66	101	84	83	666	56	7.89	2.16	3969
20	66	101	150	17	666	56	6.95	2.47	3134
20	66	101	134	33	666	56	6.15	2.71	3318
20	66	101	117	50	666	56	8.36	2.32	3562
20	66	101	101	66	666	56	12.56	2.94	3643
20	66	101	84	83	666	56	7.09	2.63	3704

References

1. Damtoft, J.S.; Lukasik, J.; Herfort, D.; Gartner, E.M. Sustainable development and climate change initiatives. *Cem. Concr. Res.* **2008**, *38*, 115–127. [CrossRef]
2. Georgescu, M.; Panait, N. Influence of CaCo3 on the hydration and hardening processes in C_3S–H_2O system. *Rom. J. Mater.* **2004**, *34*, 27–35.
3. Wi, K.; Lee, H.; Lim, S.; Song, H.; Hussin, M.; Ismail, M. Use of an agricultural by-product, nano-sized Palm Oil Fuel Ash as a supplementary cementitious material. *Constr. Build. Mater.* **2018**, *183*, 139–149. [CrossRef]
4. Keerio, M.A.; Saand, A.; Kumar, A.; Bheel, N.; Ali, A. Effect of local metakaolin developed from natural material soorh and coal bottom ash on fresh, hardened properties and embodied carbon of self-compacting concrete. *Environ. Sci. Pollut. Res.* **2021**, *28*, 60000–60018. [CrossRef] [PubMed]
5. Sakir, S.; Raman, S.N.; Safiuddin, M.; Amrul Kaish, A.B.M.; Mutalib, A.A. Utilization of By-Products and Wastes as Supplementary Cementitious Materials in Structural Mortar for Sustainable Construction. *Sustainability* **2020**, *12*, 3888. [CrossRef]
6. Kumar, R.; Shafiq, N.; Kumar, A.; Jhatial, A.A. Investigating embodied carbon, mechanical properties, and durability of high-performance concrete using ternary and quaternary blends of metakaolin, nano-silica, and fly ash. *Environ. Sci. Pollut. Res.* **2021**, *28*, 49074–49088. [CrossRef] [PubMed]
7. Revathy, J.; Yaswanth, K.K.; Gajalakshmi, P. Flexural performance of GGBS-based EGC layered reinforced cement concrete and geopolymer concrete beams: A retrofit perspective. *Innov. Infrastruct. Solut.* **2023**, *8*, 263. [CrossRef]
8. Supit, S.W.M.; Shaikh, F.U.A.; Sarker, P.K. Effect of ultrafine fly ash on mechanical properties of high volume fly ash mortar. *Constr. Build. Mater.* **2014**, *51*, 278–286. [CrossRef]
9. Praveen Kumar, V.V.; Ravi Prasada, D. Influence of supplementary cementitious materials on strength and durability characteristics of concrete. *Adv. Concr. Constr.* **2019**, *7*, 75. [CrossRef]
10. Madurwar, M.; Ralegaonkar, R.; Mandavgane, S. Application of agro-waste for sustainable construction materials: A review. *Constr. Build. Mater.* **2013**, *38*, 872–878. [CrossRef]
11. Sam, A.R.M.; Usman, J.; Sumadi, S.R. Properties of binary and ternary blended cement mortars containing palm oil fuel ash and metakaolin. *J. Chin. Inst. Eng.* **2017**, *40*, 170–178. [CrossRef]
12. Güneyisi, E.; Gesoğlu, M. Properties of self-compacting mortars with binary and ternary cementitious blends of fly ash and metakaolin. *Mater. Struct.* **2008**, *41*, 1519–1531. [CrossRef]
13. Alex, J.; Dhanalakshmi, J.; Ambedkar, B. Experimental investigation on rice husk ash as cement replacement on concrete production. *Constr. Build. Mater.* **2016**, *127*, 353–362. [CrossRef]
14. Rukzon, S.; Chindaprasirt, P. Strength, porosity, and chloride resistance of mortar using the combination of two kinds of pozzolanic materials. *Int. J. Miner. Metall. Mater.* **2013**, *20*, 808–814. [CrossRef]
15. Oruji, S.; Brake, N.A.; Nalluri, L.; Guduru, R.K. Strength activity and Microstructure of blended ultra–fine coal bottom ash–cement mortar. *Constr. Build. Mater.* **2017**, *153*, 317–326. [CrossRef]
16. Chindaprasir, P.; Ruzkon, S. Strength, porosity and corrosion resistance of ternary Portland cement, rice husk ash and fly ash mortar. *Constr. Build. Mater.* **2008**, *22*, 1601–1606. [CrossRef]
17. Nagaratnam, B.H.; Mannan, M.A.; Rahman, M.E.; Mirasa, A.K.; Richardson, A.; Nabinejad, O. Strength and microstructural characteristics of palm oil fuel ash and fly ash as binary and ternary blends in Self-Compacting concrete. *Constr. Build. Mater.* **2019**, *202*, 103–120. [CrossRef]
18. Gesoglu, M.; Guneyisi, E.; Ozbay, E. Properties of Self–Compacting Concretes made with binary, ternary and quaternary cementitious blends of Fly Ash, Blast Furnace Slag and Silica Fume. *Constr. Build. Mater.* **2009**, *23*, 1847–1854. [CrossRef]
19. Choudhary, R.; Gupta, R.; Nagar, R. Impact on fresh, mechanical, and microstructural properties of high strength self- compacting concrete by marble cutting slurry waste, fly ash, and silica fume. *Constr. Build. Mater.* **2020**, *239*, 117888. [CrossRef]
20. Dave, N.; Misra, A.K.; Srivastava, A.; Kaushik, S.K. Experimental analysis of strength and durability properties of quaternary cement binder and mortar. *Constr. Build. Mater.* **2016**, *107*, 117–124. [CrossRef]
21. Isaia, G.C.; Gastaldini, A.L.G.; Moraes, R. Physical and pozzolanic action of mineral additions on the mechanical strength of high performance concrete. *Cem. Concr. Compos.* **2003**, *25*, 69–76. [CrossRef]
22. Imam, A.; Kumar, V.; Srivastava, V. Empirical predictions for the mechanical properties of Quaternary Cement Concrete. *J. Struct. Integr. Maint.* **2018**, *3*, 183–196. [CrossRef]
23. Sivakumar, A.; Santhanam, M. Mechanical properties of high strength concrete reinforced with metallic and non-metallic fibres. *Cem. Concr. Compos.* **2007**, *29*, 603–608. [CrossRef]
24. Kanagavel, R.; Arunachalam, K. Experimental Investigation on Mechanical Properties of Hybrid Fiber Reinforced Quaternary Cement Concrete. *J. Eng. Fibers Fabr.* **2015**, *10*, 155892501501000407. [CrossRef]
25. Kumar, S.; Ganesan, N.; Indira, P.V. Engineering Properties of Hybrid Fibre Reinforced Ternary Blend Geopolymer Concrete. *J. Compos. Sci.* **2021**, *5*, 203. [CrossRef]
26. Arokiaprakash, A.; Selvan, S.S. Experimental strength evaluation of steel-polypropylene hybrid fibre reinforced concrete. *J. Eng. Res. ACMM Spec. Issue* **2022**, 1–13. [CrossRef]
27. Pickering, K.L.; Aruan Efendy, M.G.; Le, T.M. A review of recent developments in natural fibre composites and their mechanical performance. *Compos. Part A Appl. Sci. Manuf.* **2016**, *83*, 98–112. [CrossRef]

28. Poongodi, K.; Khan, A.; Mushraf, M.; Prathap, V.; Harish, G. Strength properties of hybrid fibre reinforced quaternary blended high performance concrete. *Mater. Today: Proc.* **2021**, *39*, 627–632. [CrossRef]
29. Abellan-Garcia, J.; Fernández-Gómez, J.; Khan, M.I.; Abbas, Y.M.; Pacheco-Bustos, C. ANN approach to evaluate the effects of supplementary cementitious materials on the compressive strength of recycled aggregate concrete. *Constr. Build. Mater.* **2023**, *402*, 132992. [CrossRef]
30. Ahmad, A.; Ahmad, W.; Aslam, F.; Joyklad, P. Compressive strength prediction of fly ash-based geopolymer concrete via advanced machine learning techniques. *Case Stud. Constr. Mater.* **2022**, *16*, e00840. [CrossRef]
31. Arokiaprakash, A.; Selvan, S.S. Application of Random Forest and Multi-layer Perceptron ANNS in Estimating the Axial Compression Capacity of Concrete-Filled Steel Tubes. *Iran. J. Sci. Technol. Trans. Civ. Eng.* **2022**, *46*, 4111–4130. [CrossRef]
32. Bai, J.; Wild, S.; Ware, J.A.; Sabir, B.B. Using neural networks to predict workability of concrete incorporating metakaolin and fly ash. *Adv. Eng. Softw.* **2003**, *34*, 663–669. [CrossRef]
33. Amar, M.; Benzerzour, M.; Zentar, R.; Abriak, N.-E. Prediction of the Compressive Strength of Waste-Based Concretes Using Artificial Neural Network. *Materials* **2022**, *15*, 7045. [CrossRef]
34. Mohamed, O.; Kewalramani, M.; Ati, M.; Hawat, W.A. Application of ANN for prediction of chloride penetration resistance and concrete compressive strength. *Materialia* **2021**, *17*, 101123. [CrossRef]
35. Khan, A.Q. Optimized artificial neural network model for accurate prediction of compressive strength of normal and high strength concrete. *Clean. Mater.* **2023**, *10*, 100211. [CrossRef]
36. Murthy, M.N.; Amruth, S.K.; Marulasiddappa, S.B. Modeling the compressive strength of binary and ternary blended high-performance concrete mixtures using ensemble machine learning models. *Soft Comput.* **2024**, *28*, 6683–6693. [CrossRef]
37. Lingam, A.; Karthikeyan, J. Prediction of compressive strength for HPC mixes containing different blends using ANN. *Comput. Concr.* **2014**, *13*, 621–632. [CrossRef]
38. Liu, F.; Ding, W.; Qiao, Y. An artificial neural network model on tensile behavior of hybrid steel-PVA fiber reinforced concrete containing fly ash and slag power. *Front. Struct. Civ. Eng.* **2020**, *14*, 1299–1315. [CrossRef]
39. Verma, N.K.; Meesala, C.R.; Kumar, S. Developing an ANN prediction model for compressive strength of fly ash-based geopolymer concrete with experimental investigation. *Neural Comput. Applic* **2023**, *35*, 10329–10345. [CrossRef]
40. Yaswanth, K.K.; Sathish Kumar, V.; Revathy, J.; Murali, G.; Pavithra, C. Compressive strength prediction of ternary blended geopolymer concrete using artificial neural networks and support vector regression. *Innov. Infrastruct. Solut.* **2024**, *9*, 32. [CrossRef]
41. Chepurnenko, A.; Turina, V.; Akopyan, V. Artificial Neural Network Models for Determining the Load-Bearing Capacity of Eccentrically Compressed Short Concrete-Filled Steel Tubular Columns. *CivilEng* **2024**, *5*, 150–168. [CrossRef]
42. Veerapandian, V.; Pandulu, G.; Jayaseelan, R. Simplified deep-learning approach for estimating the ultimate axial load of circular composite columns. *Asian J. Civ. Eng.* **2023**, *24*, 2375–2387. [CrossRef]
43. Demir, T.; Duranay, Z.B.; Demirel, B.; Yildirim, B. Artificial neural network evaluation of concrete performance exposed to elevated temperature with destructive–non-destructive tests. *Neural Comput. Applic* **2024**, *36*, 17079–17093. [CrossRef]
44. Raheel, M.; Khan, H.; Iqbal, M.; Khan, R.; Saberian, M.; Li, J.; Ullah, Q.S. Experimental investigation of quaternary blended sustainable concrete along with mix design optimization. *Structures* **2023**, *54*, 499–514. [CrossRef]
45. *IS 12269: 2013*; Indian Standard Methods of Specification for Ordinary Portland Cement—53 Grade. BIS: Washington, DC, USA, 2013.
46. *IS 383: 2016*; Indian Standard Specification For Coarse And Fine Aggregates From Natural Sources For Concrete. BIS: Washington, DC, USA, 2016.
47. *IS 2386 (Part 3): 1963*; Indian Standard Methods of Methods of Test for Aggregates for Concrete. BIS: Washington, DC, USA, 1963.
48. Geremew, A.; De Winne, P.; Demissie, T.A.; De Backer, H. Treatment of Natural Fiber for Application in Concrete Pavement. *Adv. Civ. Eng.* **2021**, *2021*, 6667965. [CrossRef]
49. Prasanna, K.; Anandh, K.S.; Ravi Shankar, S. An experimental study on strengthening of concrete mixed with ground granulated blast furnace slag (GGBS). *ARPN J. Eng. Appl. Sci.* **2017**, *12*, 2439–2444.
50. *IS 4031 (Part 6):1988*; Indian Standard Methods of Physical Tests for Hydraulic Cement, (Reaffirmed 2005). BIS: Washington, DC, USA, 1988.
51. *IS 5816:1999*; Indian Standard Methods of Splitting Tensile Strength of Concrete—Method of Test, (Reaffirmed 2004). BIS: Washington, DC, USA, 1999.
52. *ACI 544.2R—89: 1999*; Measurement of Properties of Fibre Reinforced Concrete. ACI: Farmington Hills, MI, USA, 1999.
53. Karthiga, S.; Umamaheswari, N. Prediction of displacement of composite slab with profiled steel deck using artificial neural network. *Asian J. Civ. Eng.* **2024**, *25*, 4179–4196. [CrossRef]
54. Yaswanth, K.K.; Revathy, J.; Gajalakshmi, P. Artificial intelligence for the compressive strength prediction of novel ductile geopolymer composites. *Comput. Concr.* **2021**, *28*, 55–68. [CrossRef]
55. Sheela, K.G.; Deepa, S.N. Review on methods to fix number of hidden neurons in neural networks. *Math. Probl. Eng.* **2013**, *2013*, 425740. [CrossRef]
56. Revathy, J.; Gajalakshmi, P.; Ashwini, G. Neural networks for the prediction of fresh properties and compressive strength of flowable concrete. *J. Urban Environ. Eng.* **2019**, *13*, 183–197. [CrossRef]
57. Albostami, A.S.; Al-Hamd, R.K.S.; Alzabeebee, S.; Minto, A.; Keawsawasvong, S. Application of soft computing in predicting the compressive strength of self-compacted concrete containing recyclable aggregate. *Asian J. Civ. Eng.* **2024**, *25*, 183–196. [CrossRef]

58. Chandramouli, P.; Jayaseelan, R.; Pandulu, G.; Sathish Kumar, V.; Murali, G.; Vatin, N.I. Estimating the Axial Compression Capacity of Concrete-Filled Double-Skin Tubular Columns with Metallic and Non-Metallic Composite Materials. *Materials* **2022**, *15*, 3567. [CrossRef] [PubMed]
59. Mala, K.; Mullick, A.K.; Jain, K.K. Effect of Relative Levels of Mineral Admixtures on Strength of Concrete with Ternary Cement Blend. *Int. J. Concr. Struct. Mater.* **2013**, *7*, 239–249. [CrossRef]
60. Elmoaty Abd, M.; Morsy, A.M.; Harraz, A.B. Effect of Fiber Type and Volume Fraction on Fiber Reinforced Concrete and Engineered Cementitious Composite Mechanical Properties. *Buildings* **2022**, *12*, 2108. [CrossRef]
61. Ismail, M.K.; Hassan, A.A.A.; Lachemi, M. Performance of Self Consolidating Engineered Cementitious Composite under Drop Weight Impact Loading. *J. Mater. Civ. Eng.* **2019**, *31*, 04018400. [CrossRef]
62. Bharatkumar, B.H.; Narayanan, R.; Raghuprasad, B.K.; Ramachandramurthy, D.S. Mix Proportioning of High Performance Concrete. *Cem. Concr. Compos.* **2001**, *23*, 71–80. [CrossRef]